Hindawi
International Journal of Aerospace Engineering
Volume 2023, Article ID 3854295, 15 pages
https://doi.org/10.1155/2023/3854295

Research Article

Aerodynamic Parameter Identification of Projectile Based on Improved Extreme Learning Machine and Ensemble Learning Theory

Tianyi Wang, Wenjun Yi, and Youran Xia

Nanjing University of Science and Technology, Nanjing, China

Correspondence should be addressed to Tianyi Wang; 573176814@qq.com

Received 11 January 2023; Revised 30 January 2023; Accepted 7 February 2023; Published 27 February 2023

Academic Editor: Binbin Yan

The firing accuracy of the projectile has a positive relation with aerodynamic parameters. Due to the complex dynamic characteristics of projectiles, there is an overfitting risk when a single extreme learning machine (ELM) is used to identify the aerodynamic parameters of the projectile, and the identification results oscillate transonic region. To obtain the aerodynamic parameters of the projectile accurately, an aerodynamic parameter identification model based on ensemble learning theory and ELM optimized by improved particle swarm optimization is proposed. The improved particle swarm optimization algorithm (IPSO) with an adaptive update strategy is used to optimize the weight and threshold of ELM. Combined with the ensemble learning theory, the improved ELM neural network is regarded as a weak learner to generate a strong learner. The structural parameters of the strong learner were continuously optimized through training, and an aerodynamic parameter identification model of projectile based on ensemble learning theory is obtained. The simulation results show that the introduction of the IPSO and ensemble learning theory enables the model to exhibit excellent generalization ability. The proposed identification model can accurately describe the variation of aerodynamic parameters with the Mach number.

1. Introduction

Aerodynamics is the decisive factor affecting the ballistic trajectory and flight stability of the projectile [1]. The projectile's firing accuracy positively relates to aerodynamic parameters [2]. Currently, numerical computation, wind tunnel test, and shooting test are common technical means to obtain aerodynamic parameters [3]. The result of the numerical calculation method depends on the accuracy of the ballistic model. Still, due to the strong coupling of the projectile flight motion and external disturbance, it is difficult to obtain a completely accurate ballistic model. The wind tunnel experiment simulates the genuine flight attitude of the projectile by changing the attitude and velocity of the model, which is generally used to test and correct the shape parameters and aerodynamic characteristics of the projectile. The parameter identification method is used to process the measured data (provided by shooting test) and indirectly extract the aerodynamic parameters of projectile. Research on the aerodynamic parameter identification method has significant practical engineering application value [4]. The least squares method (LSM), maximum likelihood method (ML), Kalman filtering method (KF), and intelligent algorithm are mature algorithms in the field of parameter identification [5–7].

LSM [8] is a classical estimation method in aircraft parameter identification. Dunkel [9] realized the identification of aerodynamic derivative and stability derivative by LSM. However, LSM is susceptible to extreme outliers. To mitigate the effects of outliers, Su and Song [10] used recursive LSM with fading memory to improve the identification performance. Kamali et al. [11] proposed improved LSM and successfully identified Dutch roll movement parameters and segment period parameters of aircraft. Mu et al. [12] combined the model reduction technology with LSM for parameter identification. Due to the complex motion characteristics of the projectile, the traditional identification equation (based on LSM) needs to be better posed. Yang et al. [13] combined LSM with an engineering test to obtain the aerodynamic parameters of projectile.

ML has been widely used due to its unbiasedness [14–17]. Carnduff and Cooke [18] applied ML to reconstruct the aerodynamic model of an unmanned aerial vehicle (UAV) with an unconventional fuselage structure. However, ML highly relies on model accuracy, and the variance is significant at high latitudes, so it is often used in combination with other methods. To improve the performance of ML, Kumar and Rao [19] combined the output error method with ML, which can accelerate the speed of convergence. Zou and Li [20] introduced the interior point optimization method into ML to reduce the severe error caused by second-order numerical differentiation.

By extending the parameters (to be identified) to system states, the problem of parameter identification can be transformed into the issue of optimal state estimation so that KF can be applied to parameter identification [21–23]. In nonlinear systems, KF cannot accurately estimate the state matrix. It was later developed into the extended Kalman filter (EKF) and unscented Kalman filter (UKF). Zheng et al. [24] proved that UKF is better than EKF in projectile parameter identification because of unscented transformation (U-transformation). To reduce the computational complexity and improve the accuracy, many other improved KF algorithms have been proposed. Menon et al. [25] combined the differential vortex lattice algorithm with EKF to realize flight path reconstruction. Majeed and Kar [26] proposed adaptive UKF to improve identification accuracy. Shen et al. [27] combined EKF with the aerodynamic semiempirical method to identify derivative residuals.

Due to the complex environment and unknown external interference, getting a completely accurate aircraft model is complex. To solve the modeling error of the traditional identification method, intelligent algorithms and their variants have been widely used in aerodynamic parameter identification. Du et al. [28] combined particle swarm optimization algorithm (PSO) with real-coded genetic algorithm (GA) to obtain the resistance coefficient of the projectile. Based on the maximum likelihood criterion, Li et al. [29] applied the neural network Newton method to extract the zero-lift drag coefficient of the projectile. To improve accuracy and accelerate convergence, Wang et al. [30] introduced an elite crossover strategy into GA. Guan et al. [31] combined GA with ML to identify the zero-lift resistance coefficient of a high-speed rotating projectile based on the speed data of the projectile. Aiming at the problem that gradient descent optimization algorithm is easy to fall into local optima in traditional aerodynamic parameter identification, Han et al. [32] put forward a double backpropagation (BP) neural network, Pu et al. [33] put forward a method of sample expansion and neural network parameter online fast correction based on support vector machine (SVM), and Li et al. [34] proposed an improved teaching-learning-based optimization (ITLBO) for aerodynamic parameter identification. To avoid the initial value estimation, Yan et al. [35] proposed a derivative method for identifying the aerodynamic parameters of aircraft by the three-layer neural network. Hou et al. [36] applied a differential evolution algorithm to weaken initial value sensitivity. Ji-gang et al. [37] combined the advantage of PSO in the initial value section and the advantages of the Newton iteration method in precise iteration and successfully identified the drag coefficient of the projectile. Mohamad et al. [38] put forward the concept of dynamic parameter estimation (DAPE).

Extreme learning machine (ELM) [39] is an algorithm for training single hidden layer feedforward neural networks (SLFNs). The structural parameters (input weights and hidden thresholds) of ELM are generated randomly and require no iterative adjustment. Owing to it, ELM has low computational complexity and good real-time performance and has been widely used in cloud computing, data visualization, and random projection [40–42]. Akusok et al. [41] applied ELM to identify the drag coefficient of the projectile for the first time. Affected by uncertain factors such as the actual combat environment and external meteorological conditions, the ballistic trajectory data is characterized by solid nonlinearity, time-dependent nature, and susceptibility to random noise. Randomly generated structural parameters lead to the oscillation of ELM identification results [42]. In addition, when a single ELM is used to identify the aerodynamic parameters of the projectile, all the given training samples are often used to model the global situation. In other words, it is easy to make insufficient use of the sample data and cause overfitting. In summary, using a single ELM to identify aerodynamic parameters has the following limitations:

(a) The identification result oscillates (especially in the transonic region) due to randomly generated structural parameters

(b) When a single ELM is used to identify projectile aerodynamic parameters, it is hard to make sufficient use of the local information of the sample data and then causes overfitting

To overcome the above problems and then accurately obtain the aerodynamic parameters of the projectile, a large number of documents are referenced. For problem (a), the classical idea is to apply PSO, GA, and other optimization algorithms to optimize the structural parameters of ELM [43–49]. However, iterative optimization increases the time complexity of the algorithm. Then, the adaptive update strategy is introduced to improve the performance of PSO. For problem (b), Schapire [50] proved that multiple weak learners could generate a strong learner with good generalization performance by ensemble theory. Considering that the projectile parameter identification problem is a regression problem, AdaBoost. RT algorithm [51] is used as the integration framework. Above all, this paper puts forward an aerodynamic parameter identification model of projectile based on improved ELM and ensemble learning theory (we named IPSO-ELM-AdaBoost). The proposed IPSO-ELM-AdaBoost is a comprehensive application of multiple algorithms. In short, the functions of the hybrid algorithm can be generalized as follows:

(a) ELM (function as a weak learner) establishes the mapping relationship between ballistic data and aerodynamic parameters

(b) Improved PSO (IPSO) provides ELM with optimized structural parameters

(c) AdaBoost. RT is responsible for integrating multiple weak learners into strong learners

The rest of the paper is arranged as follows: in Section 2, the concrete expression of the ballistic equation is given. ELM-AdaBoost. RT aerodynamic parameter identification model based on improved particle swarm optimization (IPSO-ELM-AdaBoost) is described in detail in Section 3. The simulation results under standard meteorological conditions are analyzed in Section 4. Ultimately, conclusions are summarized in Section 5.

2. Ballistic Trajectory Model

Before parameter identification, the ballistic trajectory model (6DOF) [52] must first be solved to obtain the ballistic data. 6DOF treats the projectile motion as a rigid body motion. It considers the three degrees of freedom of the projectile centroid motion and the three degrees of freedom of the angular motion. Ignoring the dynamic unbalance of the projectile, the aerodynamic eccentricity, and the Coriolis inertial force caused by the Earth's rotation, 6DOF can be mathematically described as

$$\begin{aligned}\frac{dv}{dt}=\frac{1}{m}\Bigg(&-\frac{\rho v_r}{2}Sc_{x0}\left(v-w_{x_V}\right)-\frac{\rho v_r}{2}Sc_{x2}\delta_r^2\left(v-w_{x_V}\right)\\&+\frac{\rho S}{2}c_y\frac{v_r^2\cos\delta_{lr}\cos\delta_{ud}}{\sin\delta_r}-\frac{\rho S}{2}c_y\frac{v_{r\varepsilon}\left(v-w_{x_V}\right)}{\sin\delta_r}\\&-\frac{\rho v_r}{2}Sc_z\frac{w_{z_V}\cos\delta_{lr}\sin\delta_{ud}}{\sin\delta_r}+\frac{\rho v_r}{2}Sc_z\frac{w_{y_V}\sin\delta_{lr}}{\sin\delta_r}\\&-mg\sin\theta_V\cos\psi_V,\end{aligned}\tag{1}$$

$$\begin{aligned}\frac{d\theta_V}{dt}=\frac{1}{m}\Bigg\{&\frac{\rho v_r Sc_x w_{y_V}}{2v\cos\psi_V}+\frac{\rho Sc_y\left(v_r^2\cos\delta_{lr}\sin\delta_{ud}+v_{r\zeta}w_{y_V}\right)}{2v\cos\psi_V\sin\delta_r}\\&-\frac{\rho v_r^2 Sc_y'\delta_N\cos\gamma_1}{2v\cos\psi_V}\\&+\frac{\rho v_r Sc_z\left[\left(v-w_{x_V}\right)\sin\delta_{lr}+w_{z_V}\cos\delta_{lr}\cos\delta_{ud}\right]}{2v\cos\psi_V\sin\delta_r}\\&-\frac{mg\cos\theta_V}{v\cos\psi_V}+\frac{2\Omega_E mv}{v\cos\psi_V}(\sin\psi_V\cos\theta_V\cos\Lambda\cos\alpha_d\\&+\sin\theta_V\sin\psi_V\sin\Lambda+\cos\psi_V\cos\Lambda\sin\alpha_d)\Bigg\},\end{aligned}\tag{2}$$

$$\begin{aligned}\frac{d\psi_V}{dt}=\frac{1}{m}\Bigg\{&\frac{\rho v_r}{2v}Sc_x w_{z_V}+\frac{\rho S}{2v}c_y\frac{1}{\sin\delta_r}\left[v_r^2\sin\delta_{lr}+v_{r\xi}w_{z_V}\right]\\&-\frac{\rho v^2 Sc_y'\delta_N\sin\gamma_1}{2}-\frac{\rho v_r}{2v}2c_z\frac{1}{\sin\delta_r}w_{y_V}\cos\delta_{lr}\cos\delta_{ud}\\&-\frac{\rho v_r}{2v}Sc_z\frac{1}{\sin\delta_r}\left(v-w_{x_V}\right)\cos\delta_{lr}\sin\delta_{ud}\\&+\frac{1}{v}mg\sin\theta_V\sin\psi_V+2\Omega_E m(\sin\Lambda\cos\theta_V\\&-\cos\Lambda\sin\theta_v\cos\alpha_d)\Bigg\},\end{aligned}\tag{3}$$

$$\frac{d\omega_\varepsilon}{dt}=-\frac{\rho Sld}{2C}m_{xz}'v_r\omega_\varepsilon,\tag{4}$$

$$\begin{aligned}\frac{d\omega_\eta}{dt}=\frac{1}{A}\Bigg(&\frac{\rho Sl}{2}v_r m_z\frac{1}{\sin\delta_r}v_{r\xi}-\frac{\rho Sld}{2}v_r m_{zz}'\omega_\eta\\&-\frac{\rho Sld}{2}m_y''\frac{1}{\sin\delta_r}\omega_\varepsilon v_{r\eta}-\frac{\rho v^2 Slm_z'\delta_M\sin\gamma_2}{2}\Bigg)\\&-\frac{C}{A}\omega_\varepsilon\omega_\xi+\omega_\xi^2\tan\psi_a,\end{aligned}\tag{5}$$

$$\begin{aligned}\frac{d\omega_\xi}{dt}=\frac{1}{A}\Bigg(&\frac{\rho Sl}{2}v_r m_z\frac{1}{\sin\delta_r}v_{r\eta}-\frac{\rho Sld}{2}v_r m_{zz}'\omega_\xi\\&-\frac{\rho Sld}{2}m_y''\frac{1}{\sin\delta_r}\omega_\varepsilon v_{r\xi}+\frac{\rho v^2 Slm_z'\delta_M}{2}\Bigg)\\&+\frac{C}{A}\omega_\varepsilon\omega_\eta-\omega_\eta\omega_\xi\tan\psi_a,\end{aligned}\tag{6}$$

$$\frac{d\theta_a}{dt}=\frac{\omega_\xi}{\cos\psi_a},\tag{7}$$

$$\frac{d\psi_a}{dt}=-\omega_\eta,\tag{8}$$

$$\frac{d\gamma}{dt}=\omega_\varepsilon-\omega_\xi\tan\psi_a,\tag{9}$$

$$\frac{dx}{dt}=v\cos\psi_V\cos\theta_V,\tag{10}$$

$$\frac{dy}{dt}=v\cos\psi_V\sin\theta_V,\tag{11}$$

$$\frac{dz}{dt}=v\sin\psi_V,\tag{12}$$

where v is the speed; v_r is the relative velocity; $v_{r\varepsilon}$, $v_{r\eta}$, and $v_{r\xi}$ are the components of relative velocity along ε, η, and ξ axes; x is the distance; y is the altitude; z is the lateral distance; ω_ε, ω_η, and ω_ξ are the projected components of rotational speed along ε, η, and ξ axes; θ_a is the elevation angle in coordinate system of projectile axes; S is the characteristic area; m is the mass of projectile; l is the reference projectile length; d is the reference projectile diameter; g is the acceleration of gravity;

ρ is the air density; w_{x_V}, w_{y_V}, and w_{z_V} are the projected components of wind velocity along x_V, y_V, and z_V; δ_r is the relative angle of attack; Λ is the latitude; Ω_E is the rotational angular velocity of the earth; α_d is the angle of departure; δ_r is the relative angle of attack; θ_V is the elevation angle in velocity coordinate system; ψ_V is the direction cosine in velocity coordinate system; ψ_a is the direction cosine in coordinate system of projectile axes; δ_M is the aerodynamic malalignment of additional moment; δ_N is the aerodynamic malalignment of additional force; δ_{ud} is the horizontal component of angle of attack; δ_{ld} is the longitudinal component of angle of attack; c_x is the drag coefficient; c_y is the lift coefficient; c_y' is the lift coefficient derivative; c_z is the Magnus force coefficient; m_{xz}' is the rolling damping moment coefficient derivative; m_z is the static moment coefficient; m_{zz}' is the oscillating damping moment coefficient derivative; and m_y'' is the Magnus moment coefficient derivative.

3. IPSO-ELM-AdaBoost

The proposed IPSO-ELM-AdaBoost is a comprehensive application of multiple algorithms: ELM (function as a weak learner) is used to extract aerodynamic parameters from ballistic data. PSO variants provide ELM with optimized structural parameters. AdaBoost. RT algorithm (function as an integration framework) is responsible for integrating multiple weak learners into strong learners and outputting the projectile's final aerodynamic parameter identification results. In this section, ELM and AdaBoost. RT will be briefly introduced as prior knowledge, and the idea of adaptive update strategy in IPSO will be presented in detail.

3.1. ELM. ELM [39] is a special SLFN without iterative adjustment of structural parameters. The working process of ELM can be divided into learning and prediction. For ELM with M input layer, L hidden neurons, O output layer, and activation function $\sigma(\mathbf{W}^1, \mathbf{X}, \mathbf{b})$ (the activation function can be any nonzero function), the structure of ELM is shown in Figure 1.

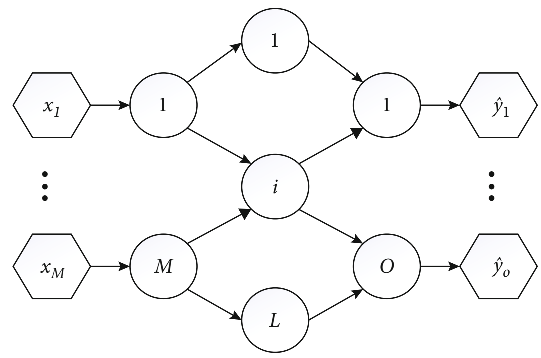

Figure 1: The structure of ELM.

3.1.1. Training Process. Given input vector $\mathbf{X}_{M\times1}$,

$$\mathbf{X}_{M\times1} = [x_1, \cdots, x_M]^T. \tag{13}$$

The structural parameters of ELM are randomly generated as follows:

$$\mathbf{W}^1_{L\times M} = \begin{bmatrix} w^1_{1,1} & \cdots & w^1_{1,M} \\ \vdots & \ddots & \vdots \\ w^1_{L,1} & \cdots & w^1_{L,M} \end{bmatrix}, \tag{14}$$

$$\mathbf{b}_{L\times1} = [b_1, \cdots, b_L]^T. \tag{15}$$

Then, the output of the hidden layer is as follows:

$$\mathbf{H}_{L\times1} = \sigma\left(\mathbf{W}^1_{L\times M} \cdot \mathbf{X}_{M\times1} + \mathbf{b}_{L\times1}\right). \tag{16}$$

The output weight matrix $\mathbf{W}^2_{O\times L}$ is mathematically described as

$$\mathbf{W}^2_{O\times L} = \begin{bmatrix} w^2_{1,1} & \cdots & w^2_{1,L} \\ \vdots & \ddots & \vdots \\ w^2_{O,1} & \cdots & w^2_{O\times L} \end{bmatrix}. \tag{17}$$

The output $\hat{\mathbf{Y}}_{O\times1}$ can be calculated as

$$\hat{\mathbf{Y}}_{O\times1} = \mathbf{W}^2_{O\times L} \cdot \mathbf{H}_{L\times1}. \tag{18}$$

Given N training samples $(\mathbf{X}_{M\times N}, \mathbf{Y}_{O\times N})$, the output of ELM is as follows:

$$\hat{\mathbf{Y}}_{O\times N} = \mathbf{W}^2_{O\times L} \cdot \mathbf{H}_{L\times N}. \tag{19}$$

The training goal is mathematically described as

$$\left\| \mathbf{Y}_{O\times N} - \hat{\mathbf{Y}}_{O\times N} \right\| = 0. \tag{20}$$

The output weight matrix can be calculated as

$$\mathbf{W}^2_{O\times L} = \mathbf{Y}_{O\times N} \cdot \mathbf{H}^+_{L\times N}, \tag{21}$$

where $\boldsymbol{H}^+_{L\times N}$ is the Moore–Penrose generalized inverse of $\mathbf{H}_{L\times N}$.

In order to improve the generalization ability of ELM and avoid overfitting, based on the ridge regression principle [53], a regularization term [54] is introduced in (21):

$$\mathbf{W}^2_{O\times L} = \mathbf{Y}_{O\times N} \cdot \left(\mathbf{H}^T_{L\times N} \cdot \mathbf{H}_{L\times N} + \frac{\mathbf{I}}{C}\right)^{-1} \cdot \mathbf{H}^T_{L\times N}, \tag{22}$$

where $\mathbf{I}$ is the identity matrix and C is the regularization factor.

3.1.2. Prediction Process. When ELM completes the training process, the output matrix $\mathbf{W}^2_{O\times L}$ can be calculated by equation (22). Given P predicting samples $\mathbf{X}_{M\times P}$, the output of ELM is

$$\hat{\mathbf{Y}}_{O\times P} = \mathbf{W}^2_{O\times L} \cdot \mathbf{H}_{L\times P}. \tag{23}$$

3.2. ISPO. PSO is a metaheuristic algorithm proposed by Kennedy and Eberhart [55]. Compared with other metaheuristic algorithms, such as GA [56] and ant colony algorithm [57], the PSO algorithm has a simple structure, easy implementation, global solid searchability, and fast convergence speed [58]. Based on the global best position $\mathbf{g}_{\text{best}}$ and the individual best position $\mathbf{p}_{\text{best}}$, the particles are iteratively updated until convergence. The steps of PSO can be described as follows:

(1) Set hyperparameter

Hyperparameters that need to be set include the following: population size e, particle dimension D, velocity inertia weight $\omega(v)$, learning factors c_1 and c_2, maximum iteration $k_{\max}$, minimum error $\Delta_{\min}$, maximum particle velocity $V_{\max}$, and maximum position $X_{\max}$.

(2) Initialization

Initialize position $\mathbf{X}_i = (x_{i1}, x_{i2}, \cdots, x_{iD})^T$ and velocity $\mathbf{V}_i = (v_{i1}, v_{i2}, \cdots, v_{iD})^T$, $i = 1, 2, \cdots e$.

(3) Iterative update

The fitness function Fitness$(\cdot)$ is selected to calculate the fitness value of particles and find out the individual and global optimum of particles. For optimization problems, the update rule is

$$\mathbf{p}_{i\text{best}}^k = \begin{cases} \mathbf{p}_{i\text{best}}^{k-1}, & \text{Fitness}\left(\mathbf{p}_{i\text{best}}^k\right) > \text{Fitness}\left(\mathbf{p}_{i\text{best}}^{k-1}\right), \\ \mathbf{X}_i^k, & \text{Fitness}\left(\mathbf{p}_{i\text{best}}^k\right) \le \text{Fitness}\left(\mathbf{p}_{i\text{best}}^{k-1}\right), \end{cases} \tag{24}$$

$$\mathbf{g}_{\text{best}}^k = \arg\ \min \left\{ \text{Fitness}\left(\mathbf{p}_{i\text{best}}^k\right) \middle| i = 1, 2, \cdots, e \right\}, \tag{25}$$

where $\mathbf{p}_{i\text{bset}}^k = (p_{i1\text{best}}^k, p_{i2\text{best}}^k, \cdots, p_{iD\text{best}}^k)^T$ specifies the individual optima of the ith particle in the kth iteration and $\mathbf{g}_{i\text{bset}}^k = (g_{1\text{best}}^k, g_{2\text{best}}^k, \cdots, g_{D\text{best}}^k)^T$ specifies global optima in the kth iteration.

Particle is iteratively updated by

$$v_{id}^{k+1} = \omega(v) v_{id}^k + c_1 r_1 \left(p_{id\text{best}}^k - x_{id}^k\right) + c_2 r_2 \left(g_{d\text{best}}^k - x_{id}^k\right), \tag{26}$$

$$x_{id}^{k+1} = x_{id}^k + v_{id}^{k+1}, \tag{27}$$

where $d = 1, 2, \cdots, D$. r_1 and r_2 are random numbers subject to uniform distribution.

(4) Iteration stop

When the algorithm converges, the optimization result is output. If not, step (3) is transferred to continue the iteration.

The structural parameters of ELM that are optimized by PSO can contain more training sample information than randomly one and can effectively improve the identification accuracy. However, the iterative optimization of PSO increases the time complexity of the algorithm. The $\omega(v)$ in equation (26) can keep the motion inertia of particles and make them tend to expand the search space, which has an important influence on the optimization performance of the algorithm. Dynamic $\omega(v)$ can obtain better optimization results than fixed one [59]. A larger $\omega(v)$ can improve the global search ability of the algorithm, while a smaller one can improve the local search ability of the algorithm. In order to improve the convergence speed of the algorithm, the adaptive update strategy is introduced in IPSO. Formula (28) calculates the average distance d_g^k from the global optimal particle to other particles in the kth iteration and then maps d_g^k to the interval [0, 1] by formula (29) to obtain the adaptive factor f. f describes the state of the population. In other words, the larger the f, the farther the particle is from the global optimal particle, and the particle needs a larger $\omega(v)$ to quickly approximate the global optimal solution. The smaller the f, the closer the particle is to the global optimal particle, and a smaller $\omega(v)$ is required to limit the particle to the vicinity of the global optimal solution and improve the search accuracy. The adaptive update strategy (based on f) of $\omega(v)$ can be described as

$$d_g^k = \frac{1}{e-1} \sum_{i=1}^{e} \left\| \mathbf{g}_{\text{best}}^k - \mathbf{X}_i^k \right\|_2, \tag{28}$$

$$f^k = \frac{d_g^k - d_{\min}^k}{d_{\max}^k - d_{\min}^k}, \tag{29}$$

$$\omega(v)^k = \left(1 - f^k\right) \omega(v)_{\min} + f^k \omega(v)_{\max}. \tag{30}$$

Table 1: Parameter setting of IPSO.

Parameter	Value
$k_{\max}$	1000
$\omega_{\max}$	0.8
$\omega_{\min}$	0.2
c_1	1.59
c_2	1.83
$V_{\max}$	0.4
$X_{\max}$	1

In order to verify the effectiveness of the IPSO, the standard test functions f_{Sp} and f_{Sc} are selected to conduct the test independently for 100 times and compared with the PSO algorithm. The expressions of test functions f_{Sp} and f_{Sc} are shown in equations (31) and (32), and the related parameter settings of the improved particle swarm are shown in Table 1. The results after 100 independent tests are given in Table 2. Test results show that the introduction of adaptive updated $\omega(v)$ in IPSO can effectively improve the

Table 2: Test results of different test functions.

Function	Algorithm	Size	Max	Min	Mean	Iteration	Theoretical value
Sphere	PSO	50	0.515	0.034	0.130	600	0
		100	0.050	0.004	0.018	400	0
		150	0.006	0.001	0.002	350	0
	IPSO	50	0.178	0.023	0.096	450	0
		100	6.35×10^{-8}	1.47×10^{-11}	5.41×10^{-9}	300	0
		150	3.83×10^{-12}	8.79×10^{-17}	6.26×10^{-13}	200	0
Schaffer	PSO	50	0.037	0.008	0.011	650	0
		100	0.037	0.009	0.010	450	0
		150	0.009	1.98×10^{-17}	0.008	400	0
	IPSO	50	0.013	0.005	0.010	500	0
		100	0.001	5.73×10^{-12}	9.14×10^{-7}	300	0
		150	1.54×10^{-5}	2.87×10^{-13}	6.27×10^{-7}	200	0

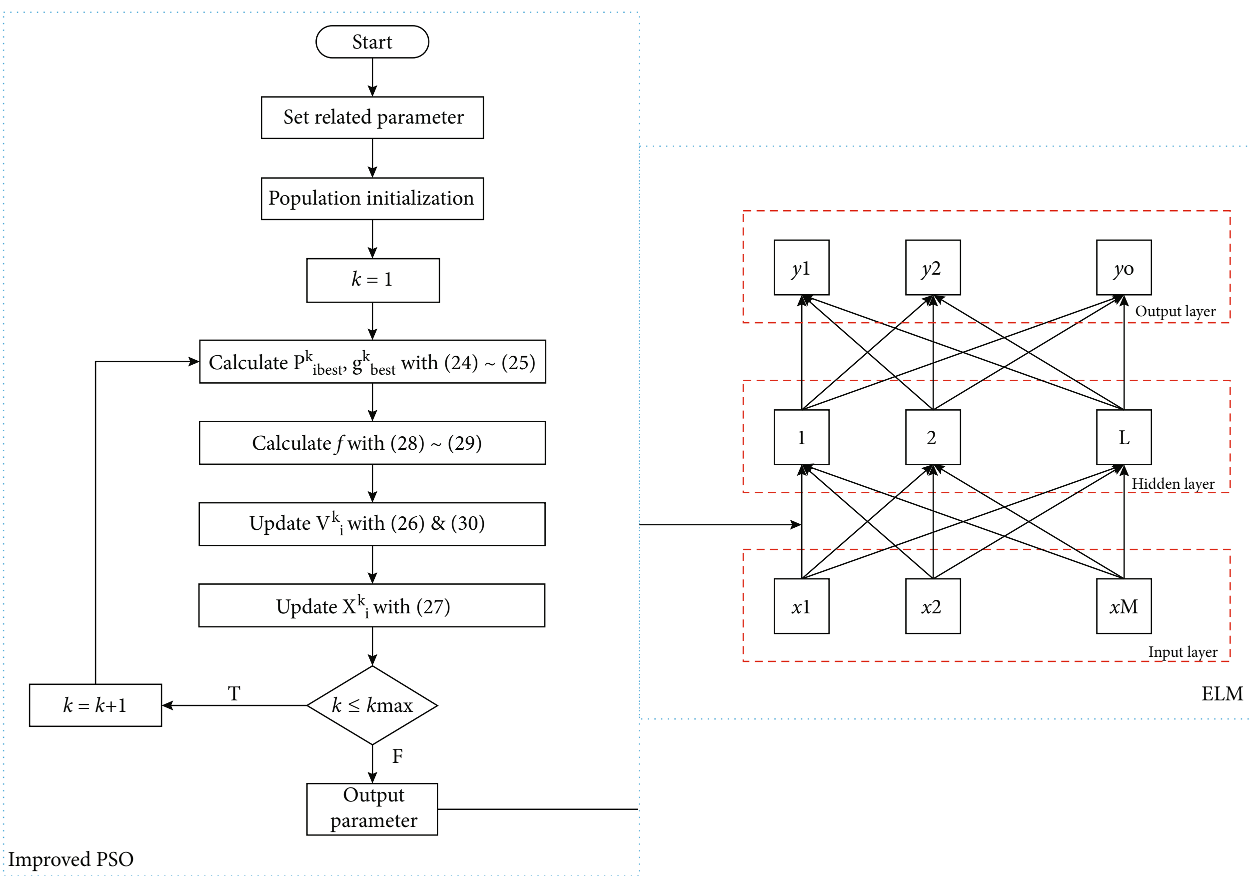

Figure 2: The structure of IPSO-ELM.

accuracy and convergence speed of the algorithm. In the case of the same number of particles, for the same test function, the results of IPSO are closer to the actual value, and the average convergence speed is faster.

$$f_{\mathrm{Sp}} = \sum_{i=1}^{30} \mu_i^2, \quad \mu_i \in [-100, 100], \tag{31}$$

$$f_{\mathrm{Sc}} = 0.5 + \frac{\left(\sin \sqrt{\mu_1^2 + \mu_2^2}\right)}{\left(1 + 0.001\left(\mu_1^2 + \mu_2^2\right)\right)^2}, \quad \mu_i \in [-10, 10]. \tag{32}$$

The structure of ELM optimized by IPSO (IPSO) is shown in Figure 2.

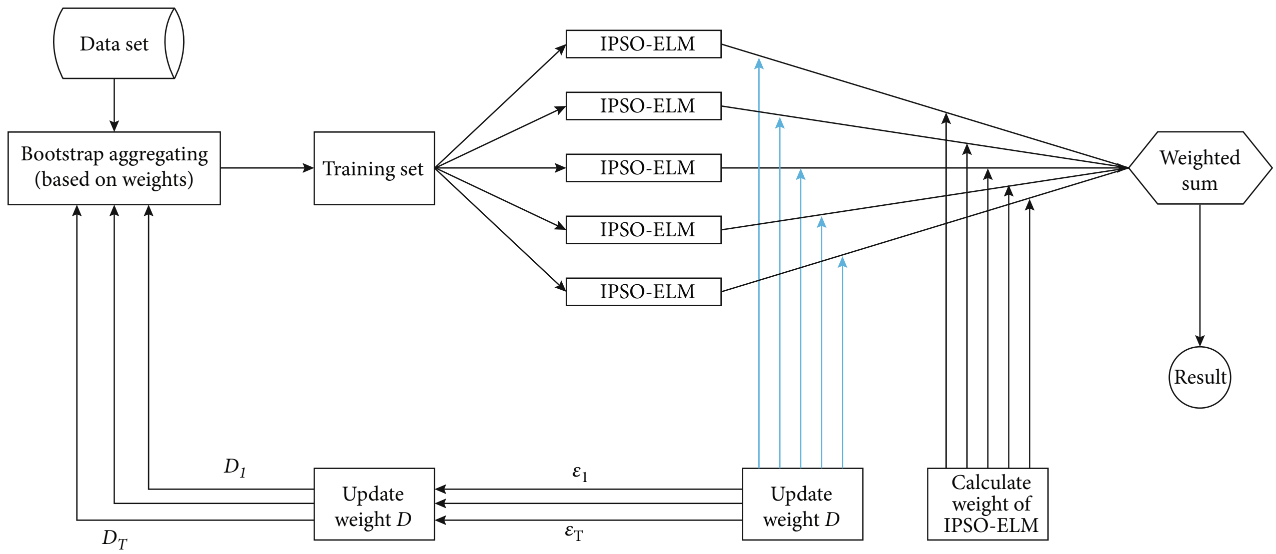

Figure 3: The structure of IPSO-ELM-AdaBoost.

3.3. AdaBoost. RT. AdaBoost. RT [60] is proposed for regression problems. The idea is to filter out examples with a relative estimation error higher than the preset threshold value and then follow the AdaBoost procedure. Its basic idea can be as follows: preset threshold φ, train weak learners (IPSO-ELM) based on training samples, and update the weight of training samples according to the current prediction error of IPSO-ELM. In the next round of training, the training samples with significant prediction error will have larger weights and continue to train weak learners based on the new weight. After M training rounds, M weak learners are obtained, and finally, the output of all weak learners is weighted to get the final prediction result. The implementation process of IPSO-ELM-AdaBoost is described as follows:

(1) Initialization

Randomly select N training samples from the dataset $\{(x_i, t_i)\}_{i=1}^N$, initialize the weight $D_j(i) = 1/N (i = 1, 2, \cdots, N)$ of the training samples, and set the threshold φ of the algorithm, the initial prediction error rate ε_1, and the iteration round number T.

(2) Train weak learners $(j \leq T)$

The jth weak learner $h_j(\cdot)$ is trained by training data, and calculate the error of each training sample (E_i^j) and weak learner (ε_j).

$$E_i^j = \left\| h_j(x_i) - t_i \right\|, \tag{33}$$

$$\varepsilon_j = \sum D_j(i), \quad i : E_i^j > \varphi, \tag{34}$$

where $h_j(x_i)$ is the prediction result of the jth weak learner (jth round) in the ith training data and t_i is the actual value.

Table 3: Initial launch parameters of 6DOF.

Initial launch parameter	Value
v_0 (m/s)	930
θ_a (°)	45
ψ_a (°)	95
ω_0 (rad/s)	188.5

(3) Update the weight of training samples

The updated formula is as follows:

$$D_{j+1}(i) = \begin{cases} \left[\dfrac{D_j(i)}{B_j}\right] \cdot \varepsilon_j^2, & E_i^j \leq \varphi, \\ \left[\dfrac{D_j(i)}{B_j}\right] \cdot \left(\dfrac{1}{\varepsilon_j^2}\right), & E_i^j > \varphi, \end{cases} \tag{35}$$

where B_j is the normalization factor.

(4) Repeat the training

Repeat T rounds of the step to obtain T weak learners and weighting to obtain the output of the strong learner:

$$h(x) = \frac{\sum_{j=1}^T \left[\ln\left(1/\varepsilon_t^2\right) h_j(x)\right]}{\sum_{j=1}^T \ln\left(1/\varepsilon_t^2\right)}. \tag{36}$$

The flow chart of IPSO-ELM-AdaBoost is shown in Figure 3.

4. Simulation Verification

In this section, a series of simulation tests are carried out under standard weather conditions to validate the feasibility

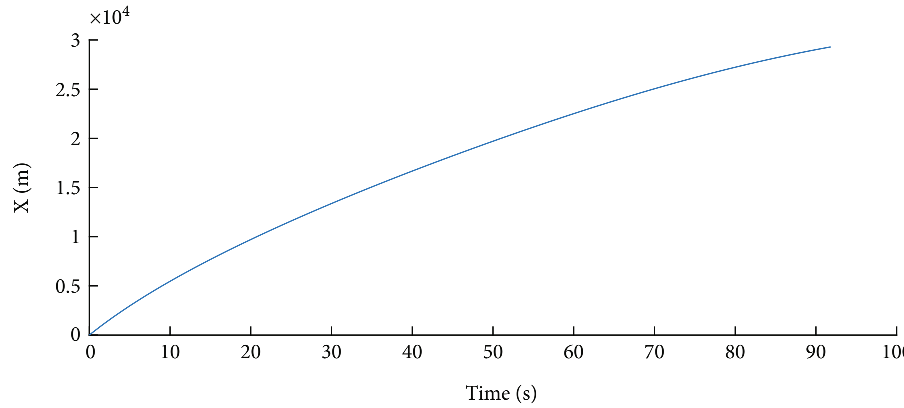

Figure 4: X-T curve.

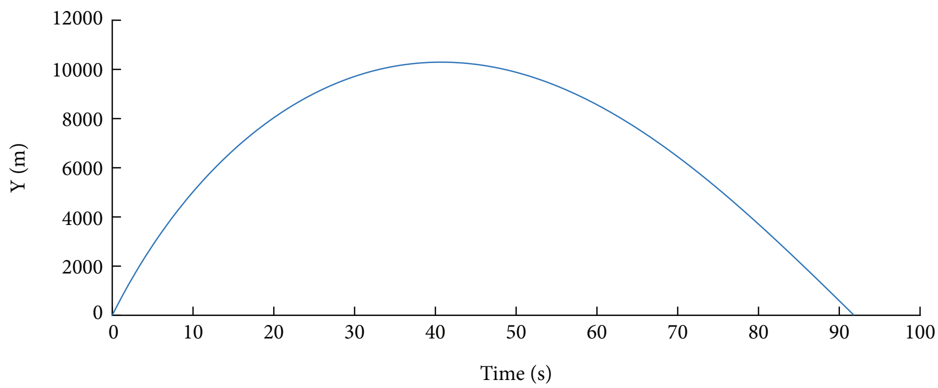

Figure 5: Y-T curve.

and excellence of IPSO-ELM-AdaBoost in aerodynamic parameter identification. In simulation test 1, IPSO-ELM-AdaBoost is compared with three other machine learning algorithms (ELM, IPSO-ELM, and ELM-AdaBoost), and the performance of mentioned machine learning algorithms is stated in the quantitative ways. In simulation test 2, IPSO-ELM-AdaBoost, LSM, ML, and UKF are used to reconstruct the trajectory, respectively. The performance of the four algorithms is evaluated from the point of fall and side deflection.

4.1. Data Preprocessing. Under standard meteorological conditions, 6DOF in Section 2 is solved, and 10000 ballistic data are obtained. Table 3 shows the initial launch parameters of 6DOF, and the variation laws of the X, Y, Z, and V of the projectile with time are shown in Figures 4–7.

The ballistic trajectory data contains the flight velocity, position, and attitude of the projectile, and different information has different dimensions. To eliminate the influence of different dimensions on data analysis, the min-max normalization is used to preprocess 10000 original datasets. The formula is as follows:

$$x_j^* = \frac{x_j - x_{\min}}{x_{\max} - x_{\min}}, \quad (37)$$

where x_j represents the original data, $x_{\min}$ is the minimum value of data, $x_{\max}$ represents the maximum value of data, and x_j^* represents the normalized data.

4.2. Simulation Test 1. Figures 8–12 are graphs of aerodynamic parameter identification results. In the figure, the abscissa represents the Mach number (Ma), and the ordinate represents aerodynamic parameters to be identified. The identification result of IPSO-ELM-AdaBoost can accurately fit the real aerodynamic parameter curves in the whole trajectory range. For the same parameter to be identified, the introduction of the IPSO and ensemble learning theory enables the model to exhibit excellent generalization ability. Take the identification results of m_{xz}' (Figure 12) as an example, the identification result curve of ELM oscillates, especially in the transonic region $(0.8 < \mathrm{Ma} < 1.2)$. The identification results of IPSO-ELM and ELM show that the structural parameters optimized by IPSO contain more sample information, which leads to higher curve fitting degree. Comparing the identification results of ELM-AdaBoost and ELM, it is found that the identification result curve considering multiple weak learners can better describe the variation law of aerodynamic parameters with Ma. It is worth mentioning that (by comparing the identification results of IPSO-ELM and ELM-AdaBoost), although IPSO

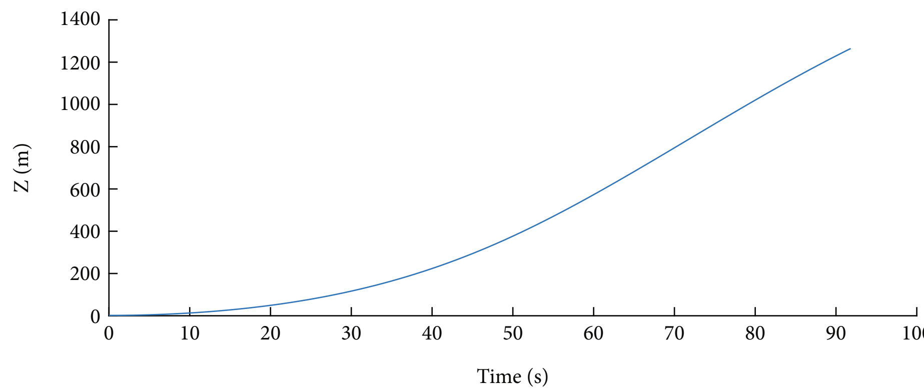

Figure 6: Z-T curve.

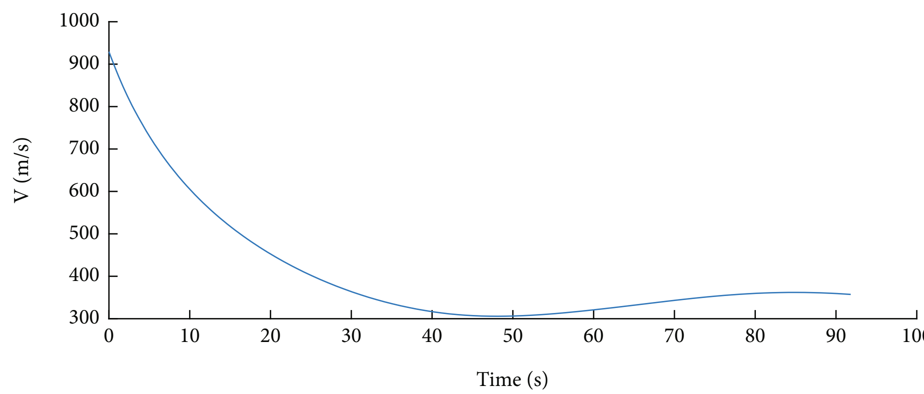

Figure 7: V-T curve.

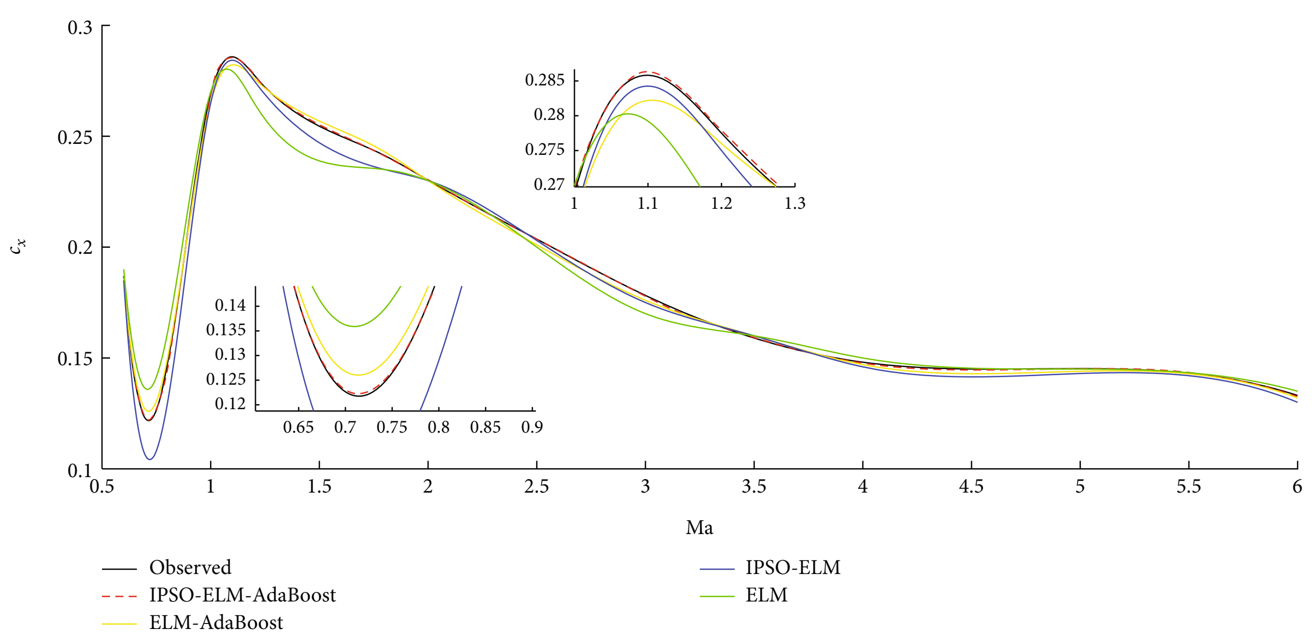

Figure 8: Identification results of c_x.

can improve the performance of the model, respectively, ISPO-ELM still has the risk of overfitting because it only takes a single learner into consideration. For different aerodynamic parameters (to be identified), the linearity between aerodynamic parameters and Ma affects the fitting degree. The stronger the linearity between aerodynamic parameters

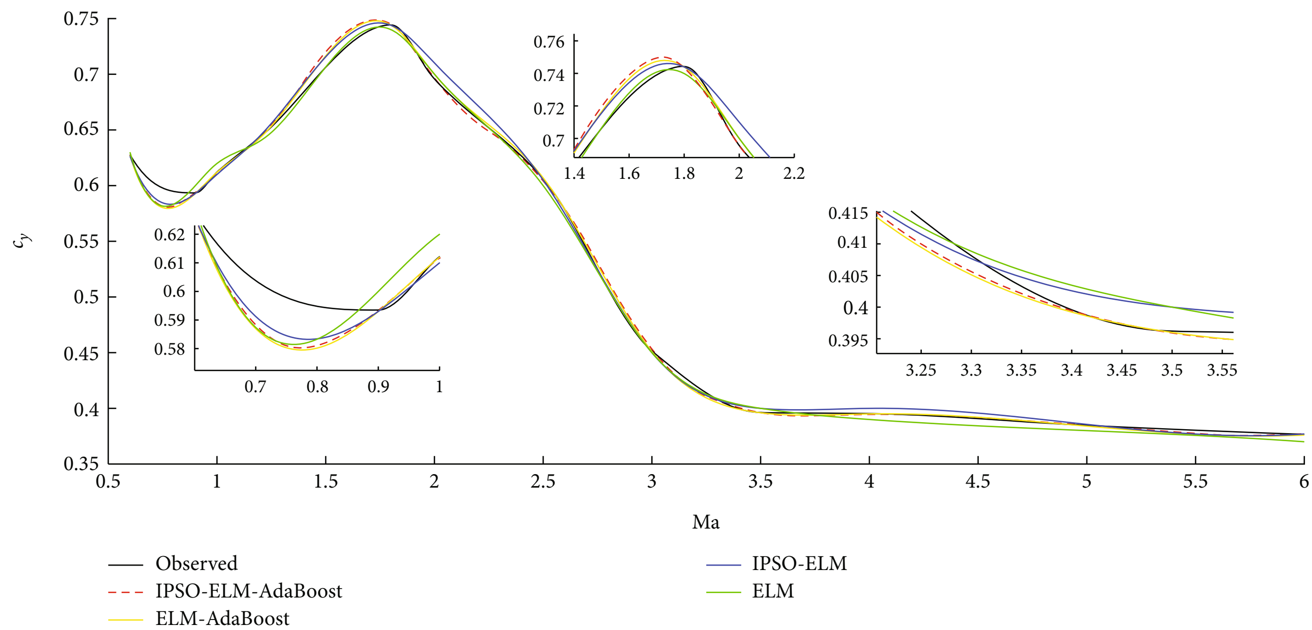

Figure 9: Identification results of c_y.

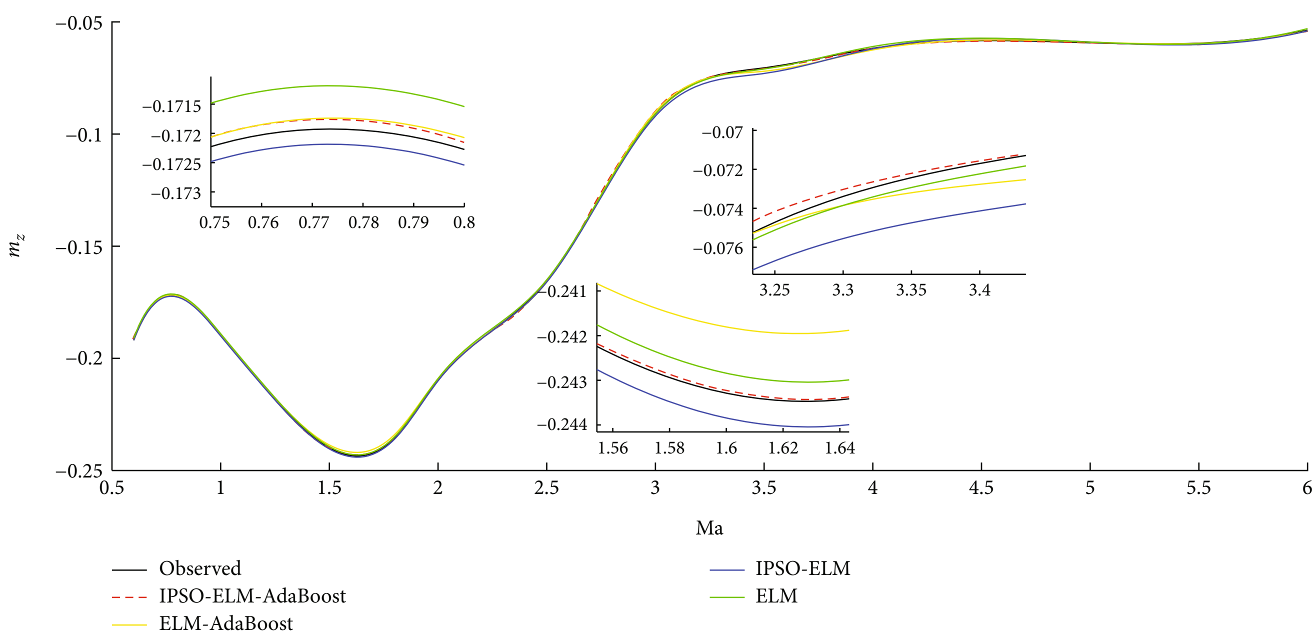

Figure 10: Identification results of m_z.

to be identified and Ma, the higher the curve fitting degree of identification results.

Table 4 shows the model structure and average identification time (after 100 independent tests) of the four algorithms. From the perspective of model structure, the introduction of IPSO and ensemble learning theory can effectively reduce the number of neurons in the hidden layer and simplify the model. From the point of identification time, although the IPSO algorithm and the introduction of ensemble learning theory simplify the complexity of the model, the iterative optimization process of IPSO and the serial training process of the weak learner by AdaBoost. RT both lead to the increase in identification time.

To further assess the performance of the model, three well-known measures are taken [61–64]. The description of these measures is as follows:

(a) *Correlation Coefficient* (R). R is a statistical measure of the strength of a linear relationship between two variables. Its values can range $[-1, 1]$. $R = 1$ shows a perfect positive correlation, or a direct relationship. $R = -1$ describes a perfect negative, or inverse,

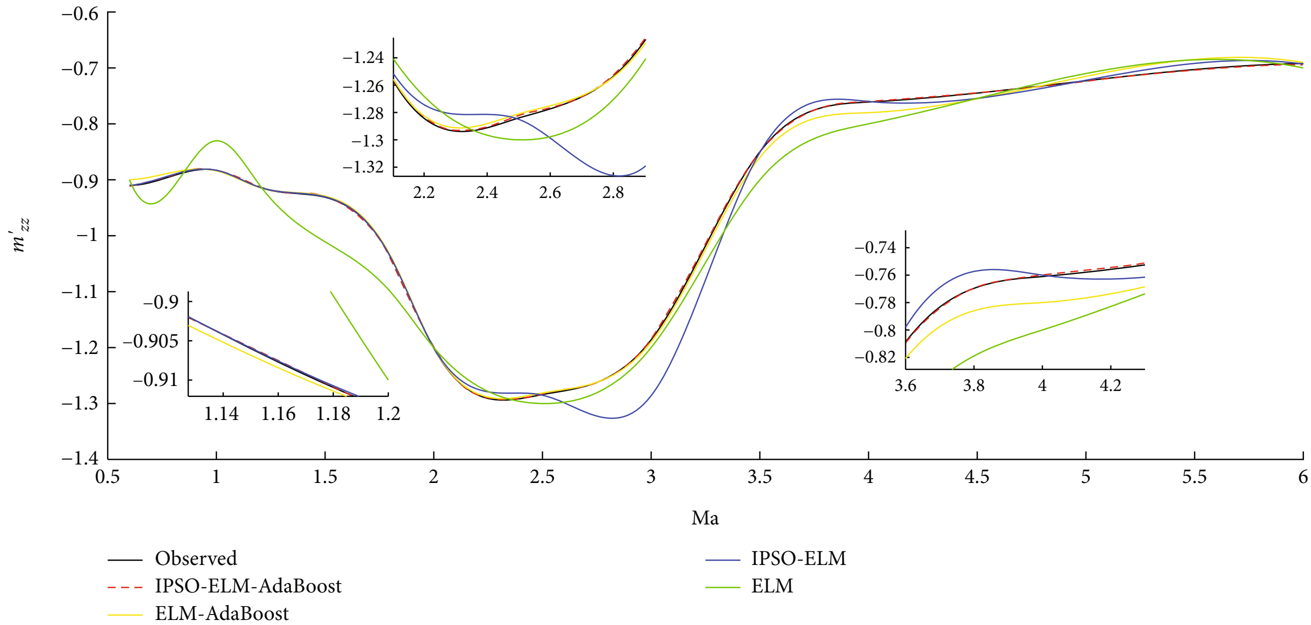

Figure 11: Identification results of m'_{zz}.

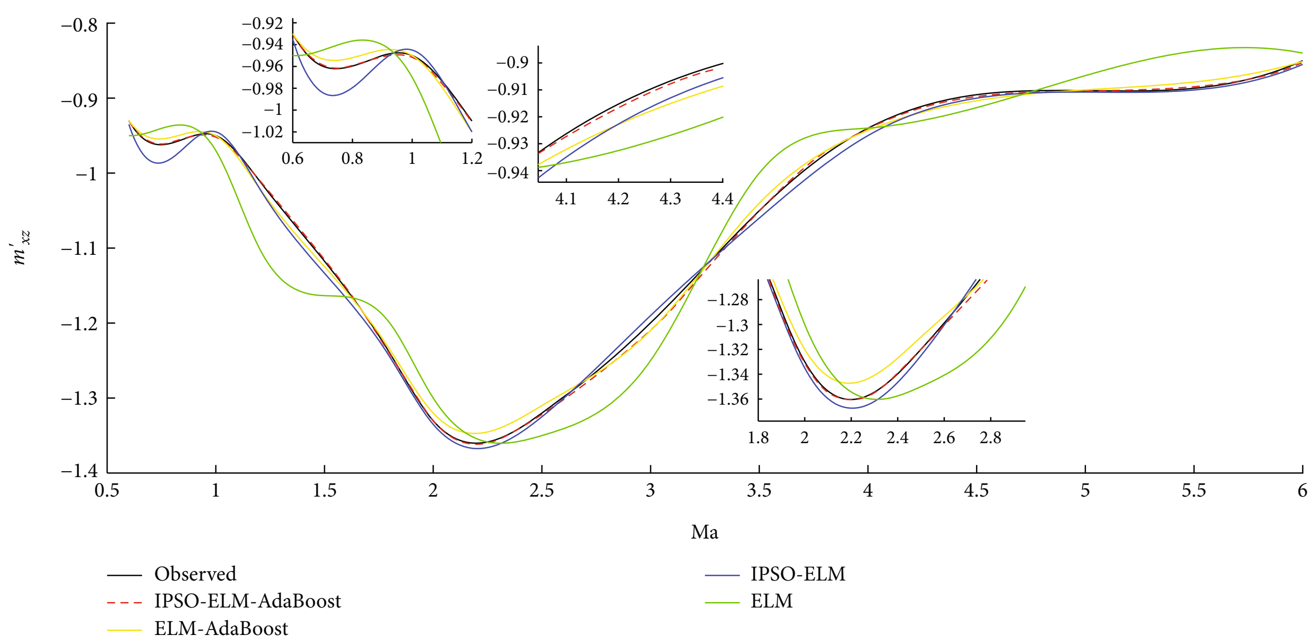

Figure 12: Identification results of m'_{xz}.

Table 4: Results of four algorithms.

Model	Structure	Time (s)
ELM	12-95-5	8.7
IPSO-ELM	12-70-5	20.3
ELM-AdaBoost	12-65-5	31.9
IPSO-ELM-AdaBoost	12-50-5	33.5

correlation, with values in one series rising as those in the other decline and vice versa. Moreover, when $R = 0$, there is no possible agreement between experimental results and numerical ones

(b) *Mean Square Error (MSE)*. As a common model performance evaluation function, MSE can reflect the difference between the observed and the predicted ones. The smaller the order of magnitude of MSE, the higher the identification accuracy

Table 5

(a) R of four algorithms

	c_x	c_y	m_z	m'_{zz}	m'_{xz}
ELM	0.61	0.75	0.89	0.16	0.14
IPSO-ELM	0.72	0.77	0.92	0.57	0.62
ELM-AdaBoost	0.83	0.81	0.94	0.89	0.86
IPSO-ELM-AdaBoost	0.90	0.85	0.97	0.92	0.91

(b) MSE of four algorithms

	c_x	c_y	m_z	m'_{zz}	m'_{xz}
ELM	7.59×10^{-3}	9.10×10^{-7}	6.44×10^{-14}	2.96×10^{-3}	3.63×10^{-3}
IPSO-ELM	6.47×10^{-4}	1.31×10^{-7}	3.17×10^{-14}	5.81×10^{-5}	1.58×10^{-6}
ELM-AdaBoost	3.20×10^{-10}	5.36×10^{-10}	9.44×10^{-16}	1.03×10^{-9}	1.54×10^{-10}
IPSO-ELM-AdaBoost	7.59×10^{-11}	4.83×10^{-11}	2.84×10^{-16}	8.30×10^{-10}	1.07×10^{-10}

(c) MAPE (%) of four algorithms

	c_x	c_y	m_z	m'_{zz}	m'_{xz}
ELM	25.8	28.4	9.6	55.2	71.2
IPSO-ELM	29.6	23.9	5.5	47.7	15.9
ELM-AdaBoost	10.2	20.7	5.8	10.3	9.2
IPSO-ELM-AdaBoost	7.1	18.4	4.1	10.0	8.3

(c) *Mean Absolute Percentage Error (MAPE)*. MAPE is a relative error measure that uses absolute values to avoid positive and negative errors canceling out. For each data series, MAPE value is a positive ratio of error value (difference between predicted output and observed one) to observed value

The specific expression of the above-mentioned measures can be described as

$$R = \frac{\sum_{t=1}^{P}\left(\text{predicted}_t - \overline{\text{predicted}}\right)\left(\text{observed}_t - \overline{\text{observed}}\right)}{\sqrt{\sum_{t=1}^{P}\left(\text{predicted}_t - \overline{\text{predicted}}\right)^2 \sum_{t=1}^{P}\left(\text{observed}_t - \overline{\text{observed}}\right)^2}}, \tag{38}$$

$$\text{MSE} = \frac{1}{P}\sum_{t=1}^{P}\left(\text{observed}_t - \text{predicted}_t\right)^2, \tag{39}$$

$$\text{MAPE} = \frac{100}{P}\sum_{t=1}^{P}\left|\frac{\text{predicted}_t - \text{observed}_t}{\text{observed}_t}\right|, \tag{40}$$

where P represents the number of predicted samples, observed_t represents the tth actual observation value, predicted_t represents the tth model prediction value, $\overline{\text{predicted}_t}$ is the mean of predicted_t, and $\overline{\text{observed}_t}$ is the mean of observed_t.

The statistical results are collected in Table 5. Under the combined action of ensemble theory and structural parameters (optimized by IPSO), IPSO-ELM-AdaBoost has the best generalization performance among the four machine learning algorithms. The structural parameters of ELM optimized by IPSO can make the input weight and threshold contain more information of input samples, which can effectively improve the identification accuracy. AdaBoost can also improve the identification accuracy by comprehensively considering the learning results of multiple weak learners. The results of IPSO-ELM and ELM-AdaBoost show that ensemble theory improves more on the performance of the algorithm. This is because structural parameters (optimized by IPSO) contain more sample information, but on the other hand, they also increase the risk of overfitting.

4.3. Simulation Test 2. In order to further verify the excellent performance of the proposed algorithm in projectile aerodynamic parameter identification, IPSO-ELM-AdaBoost is compared with the traditional projectile parameter identification algorithm (LSM, ML, and UKF). Figure 13 shows the trajectory reconstruction results of the four algorithms. The trajectory reconstructed by IPSO-ELM-AdaBoost has the highest fitting degree with the actual trajectory. Among the three traditional algorithms, the reconstructed result of UKF is the closest to the actual trajectory. The fitting degree of the four algorithms from low to high is as follows: LSM, ML, UKF, and IPSO-ELM-AdaBoost. In practical engineering, more attention is paid to the landing point and side deflection of the projectile, so the landing point (X) and side deflection (Z) of the four algorithms are also presented in

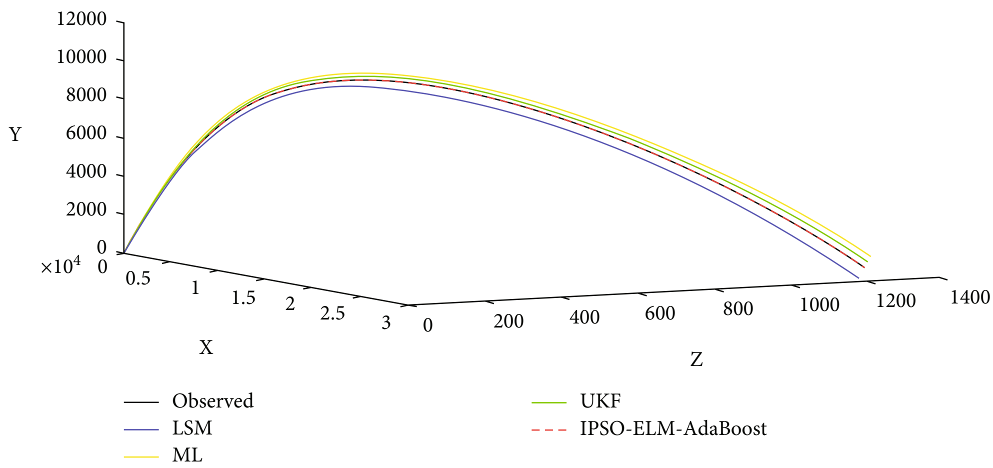

Figure 13: Results of ballistic reconstructions.

Table 6: Results of four algorithms.

	X (m)	Z (m)
Observed	29013	1230
LSM	29127 (+114)	1213 (-17)
ML	28952 (-61)	1247 (+17)
UKF	28980 (+33)	1239 (+9)
IPSO-ELM-AdaBoost	29019 (+6)	1228 (-2)

Table 6. Compared with the traditional algorithm, the proposed algorithm has the highest accuracy. The drop point error of IPSO-ELM-AdaBoost is 6 m, and the sideway error is 2 m. In terms of the drop point error, the drop point error of LSM and ML is more than 50 meters, which can no longer meet the need of actual engineering. From the perspective of side deviation error, UKF and IPSO-ELM-AdaBoost have good performance, and their side deviation error is less than 10 m.

5. Conclusion

Accurate aerodynamic parameters can effectively improve the firing accuracy of the projectile. Affected by uncertain factors such as actual combat environment and external meteorological conditions, the actual ballistic trajectory data is characterized by strong nonlinearity, time-dependent nature, and susceptibility to random noise. Take a single ELM for aerodynamic parameters, and the identification result curve oscillates in transonic region. To accurately obtain aerodynamic parameters of projectile, a new aerodynamic parameter identification model based on improved ELM and ensemble theory is constructed. Under standard weather conditions, the model is trained by trajectory data, and the mapping relationship between trajectory data and aerodynamic parameters is established. The simulation results show that the generalization ability of the model can be effectively improved by optimizing the structural parameters of ELM with IPSO and integrating several weak learners into one strong learner. Although the identification time is increased because of the iterative optimization of IPSO and serial training of AdaBoost. RT, the identification time of IPSO-ELM-AdaBoost is still the same order as that of ELM. The proposed IPSO-ELM-AdaBoost has excellent performance in the aerodynamic parameter identification of projectile and can be extended to the other aircraft.

Data Availability

The data that support the findings of this study are available from the corresponding author upon reasonable request.

Conflicts of Interest

The authors declare that there are no conflicts of interest regarding the publication of this paper.

References

[1] X. Qian, R. Lin, and Y. Zhao, *Missile Flight Mechanics*, Beijing Institute of Technology Press, Beijing, 2020.

[2] G. Yan and Z. Qi, *Marking Technique*, National Defense Industry Press, Beijing, 2000.

[3] W. Wei, *Analysis of Characteristic Parameter Method of Missile and Arrow Free Flight Test Data Identification*, Nanjing University of Science and Technology, 2009.

[4] H. Kun, *Research on Aerodynamic Parameter Identification Technology of Rocket*, North University of China, 2015.

[5] L. Lin, *Research on Aerodynamic Parameter Identification Technology of Projectile and Arrow*, North University of China, 2016.

[6] J. S. Cai, "Progress in aerodynamic parameter identification of aircraft," *Advances in mechanics*, vol. 4, pp. 467–478, 1987.

[7] F. Xu, *Research on Identification Method of Aerodynamic Parameters of Projectile and Arrow Based on Combined Measurement of Projectile and Load*, Nanjing University of Science and Technology, 2019.

[8] J. W. Liu, "Application of least square method in system identification," *Journal of Beijing Institute of Civil Engineering and Architecture*, vol. 20, no. 3, pp. 19–22, 2004.

[9] W. Dunkel, “Identification of a nonlinear model for state estimation in an airplane,” *IFAC Proceedings Volumes*, vol. 25, no. 15, pp. 553–559, 1992.

[10] H. Su and S. Song, “A better on-line identification algorithm with impairment of aircraft control surfaces considered,” *Journal of Northwestern Polytechnical University*, vol. 23, no. 3, p. 320, 2005.

[11] C. Kamali, A. A. Pashilkar, and J. R. Raol, “Evaluation of recursive least squares algorithm for parameter estimation in aircraft real time applications,” *Aerospace Science and Technology*, vol. 15, no. 3, pp. 165–174, 2011.

[12] T. Mu, L. Zhou, Y. Yang, and J. N. Yang, “Parameter identification of aircraft thin-walled structures using incomplete measurements,” *Journal of Vibroengineering*, vol. 14, no. 2, pp. 602–610, 2012.

[13] Y. G. Yang, J. M. Zhao, J. S. Liu, K. Wang, G. Wang, and Q. Wang, “Engineering algorithm of missile parameter identification based on least square method,” *Journal of Projectiles, Rockets, Misslie and Guidance*, vol. 38, no. 4, pp. 77–80, 2018.

[14] R. Jategaonkar, D. Fischenberg, and W. V. Gruenhagen, “Aerodynamic modeling and system identification from flight data-recent applications at DLR,” *Journal of Aerospace Sciences & Technologies*, vol. 41, no. 4, pp. 681–691, 2004.

[15] K. C. Wang and K. W. Iliff, “Retrospective and recent examples of aircraft parameter identification at NASA Dryden Flight Research Center,” *Journal of Aircraft*, vol. 41, no. 4, pp. 752–764, 2004.

[16] E. A. Morelli and V. Klein, “Application of system identification to aircraft at NASA Langley Research Center,” *Journal of Aircraft*, vol. 42, no. 1, pp. 12–25, 2005.

[17] N. K. Gupta and W. E. Hall, “Design and evaluation of sensor systems for state and parameter estimation,” *Journal of Guidance and Control*, vol. 1, no. 6, pp. 397–403, 1978.

[18] S. Carnduff and A. Cooke, “Application of aerodynamic model structure determination to UAV data,” *Aeronautical Journal*, vol. 115, no. 1170, pp. 481–492, 2011.

[19] N. S. Kumar and N. J. Rao, “Estimation of stability and control derivatives of light canard research aircraft from flight data,” *Defence Science Journal*, vol. 54, no. 3, pp. 277–292, 2004.

[20] X. Zou and C. Li, “Maximum likelihood method based on interior point algorithm for aircraft parameter identification,” *Journal of Aircraft*, vol. 42, no. 5, pp. 1355–1358, 2005.

[21] P. Eykhoff, *Translated by Pan Keyan et al. System Identification: Parameter and State Estimation*, Science Press, Beijing, 1980.

[22] J. Garciavelo and B. K. Walker, “Aerodynamic parameter estimation for high-performance aircraft using extended Kalman filtering,” *Journal of Guidance Control & Dynamics*, vol. 20, no. 6, pp. 1257–1260, 1997.

[23] H. S. Lee, W. S. Ra, J. G. Lee, Y. K. Song, and I. H. Whang, “Aerodynamic derivatives identification using a non-conservative robust Kalman filter,” *Journal of Electrical Engineering and Technology*, vol. 7, no. 1, pp. 132–140, 2012.

[24] Y. C. Zheng, W. J. Yi, C. H. Yu, and J. Guan, “Identification of high-spinning projectile drag coefficient using two kinds of Kalman filter,” *Journal of Ordnance Equipment Engineering*, vol. 39, no. 7, pp. 45–49, 2018.

[25] P. K. Menon, P. Sengupta, S. Vaddi, B. J. Yang, and J. Kwan, “Impaired aircraft performance envelope estimation,” *Journal of Aircraft*, vol. 50, no. 2, pp. 410–424, 2013.

[26] M. Majeed and I. N. Kar, “Aerodynamic parameter estimation using adaptive unscented Kalman filter,” *Aircraft Engineering and Aerospace Technology*, vol. 85, no. 4, pp. 267–279, 2013.

[27] J. Shen, Y. Su, Q. Liang, and X. Zhu, “Calculation and identification of the aerodynamic parameters for small-scaled fixed-wing UAVs,” *Sensors*, vol. 18, no. 2, p. 206, 2018.

[28] C. Du, H. Sun, D. Zhou, and B. Song, “Trajectory parameter identification method based on particle swarm optimization,” *Fire and command and control*, vol. 34, no. 7, pp. 162–164, 2009.

[29] J. S. Li, S. J. Chang, and S. F. Chen, “Identification of projectile drag coefficient based on neural network algorithm,” *Journal of Ballistics*, vol. 30, no. 4, pp. 38–43, 2018.

[30] Y. Wang, X. Qi, H. Zhang, and J. Qiu, “Research on aerodynamic parameter identification of power parachute based on improved genetic algorithm,” *Computer simulation*, vol. 6, pp. 37–40, 2015.

[31] J. Guan, W. Yi, H. Liu, S. Chang, J. Shi, and S. Liu, “Identification of drag coefficient of high-speed rotating projectile based on genetic maximum likelihood method,” *Ballistic journal*, vol. 4, pp. 1–6, 2016.

[32] J. Han, D. Changping, Z. Ye, G. Song, and Y. Zheng, “Aerodynamic parameter identification of ornithopter based on double BP neural network,” *Computer application*, vol. 39, no. 4, 2019.

[33] J. Pu, Y. Han, and L. Zhang, “Research on intelligent on-line identification technology of aerodynamic parameters of aircraft,” *Total aerospace technology*, vol. 6, no. 9, 2018.

[34] F. Li, C. Min, and P. Zhang, “Aerodynamic parameter identification of model free flight based on improved TLBO algorithm,” *Flight mechanics*, vol. 37, no. 169(05), pp. 84–89, 2019.

[35] C. Yan, Y. Tong, and J. Song, “Two methods for aircraft aerodynamic parameter identification based on feedforward neural network,” *Missiles and Space Vehicles*, vol. 6, p. 6, 2020.

[36] X. Hou, L. Wang, and J. fu, “Application of differential evolution intelligent algorithm in aerodynamic identification of high-spin bombs,” *Journal of Missile, Arrow and Guidance*, vol. 40, no. 3, p. 5, 2020.

[37] J. G. Shi, W. J. Yi, J. Guan, and S. P. Liu, “Drag coefficient identification of spinning projectile using particle swarm Newton iteration method,” *Journal of Ordnance Equipment Engineering*, vol. 2, pp. 23–26, 2017.

[38] A. Mohamad, J. Karimi, and A. Naderi, “Dynamic aerodynamic parameter estimation using a dynamic particle swarm optimization algorithm for rolling airframes,” *Journal of the Brazilian Society of Mechanical Sciences and Engineering*, vol. 42, no. 11, 2020.

[39] G. B. Huang, Q. Y. Zhu, and C. K. Siew, “Extreme learning machine: theory and applications,” *Neurocomputing*, vol. 70, no. 1-3, pp. 489–501, 2006.

[40] J. Lin, J. Yin, X. Zhang, Z. Cai, and Y. Ming, “Optimization mechanism for secure outsourcing extreme learning machine in cloud computing,” *Computer & Digital Enigneering*, vol. 4, no. 1, pp. 157–160, 2019.

[41] A. Akusok, S. Baek, Y. Miche et al., “ELMVIS+: fast nonlinear visualization technique based on cosine distance and extreme learning machines,” *Neurocomputing*, vol. 205, pp. 247–263, 2016.

[42] Y. Xia, W. Yi, and D. Zhang, “Coupled extreme learning machine and particle swarm optimization variant for projectile aerodynamic identification,” *Engineering Applications of Artificial Intelligence*, vol. 114, article 105100, 2022.

[43] C. Chen, C.-M. Vong, C.-M. Wong, W. Wang, and P.-K. Wong, "Efficient extreme learning machine via very sparse random projection," *Soft Computing*, vol. 22, no. 11, pp. 3563–3574, 2018.

[44] K. Yan, S. X. Li, L. Li, and Y. R. Xia, "Projectile resistance coefficient identification based on extreme learning machine," *Journal of Ballistics*, vol. 34, no. 1, pp. 31–37, 2022.

[45] Z. Lian, L. Duan, Y. Qiao, J. Chen, J. Miao, and M. Li, "The improved ELM algorithms optimized by bionic WOA for EEG classification of brain computer interface," *IEEE Access*, vol. 9, pp. 67405–67416, 2021.

[46] J. Cheng, J. Chen, Y. N. Guo, S. Cheng, L. Yang, and P. Zhang, "Adaptive CCR-ELM with variable-length brain storm optimization algorithm for class-imbalance learning," *Natural Computing*, vol. 20, no. 1, pp. 11–22, 2021.

[47] K. Kumar and N. Bhalaji, *A Novel Hybrid RNN-ELM Architecture for Crime Classification*, American Library Association, Chicago, 2020.

[48] L. Yang and Q. Zhao, "A novel PPA method for fluid pipeline leak detection based on OPELM and bidirectional LSTM," *IEEE Access*, vol. 8, pp. 107185–107199, 2020.

[49] Y. P. Gan, L. Y. Wu, K. J. Wang, B. Chen, and J. Guan, "Optimization of bomb aerodynamic parameter identification based on genetic algorithm for extreme learning machine," *Journal of Ordnance Equipment Engineering*, vol. 43, no. 9, pp. 250–256, 2022.

[50] R. E. Schapire, "The strength of weak learnability," *Machine Learning*, vol. 5, no. 2, pp. 197–227, 1990.

[51] D. L. Shrestha and D. P. Solomatine, "Experiments with AdaBoost.RT, an improved boosting scheme for regression," *Neural Computation*, vol. 18, no. 7, pp. 1678–1710, 2006.

[52] Z.-P. Han, *Exterior Ballistics of Projectiles and Rockets*, Beijing Institute of Technology Press, Beijing, China, 2014.

[53] A. E. Hoerl and R. W. Kennard, "Ridge regression: biased estimation for nonorthogonal problems," *Technometrics*, vol. 42, no. 1, pp. 80–86, 2000.

[54] G. Huang, G. B. Huang, S. Song, and K. You, "Trends in extreme learning machines: a review," *Neural Networks*, vol. 61, pp. 32–48, 2015.

[55] J. Kennedy and R. Eberhart, "Particle swarm optimization," in *Proceedings of ICNN'95 - International Conference on Neural Networks*, Perth, WA, Australia, 1995.

[56] R. Urraca, E. Sodupe-Ortega, J. Antonanzas, F. Antonanzas-Torres, and F. J. Martinez-de-Pison, "Evaluation of a novel GA-based methodology for model structure selection: the GA-PARSIMONY," *Neurocomputing*, vol. 271, pp. 9–17, 2018.

[57] Y. Wu, M. Gong, W. Ma, and S. Wang, "High-order graph matching based on ant colony optimization," *Neurocomputing*, vol. 328, pp. 97–104, 2019.

[58] S. Chen, Y. Yuan, and J. Wang, "An adaptive latent factor model via particle swarm optimization for high-dimensional and sparse matrices," in *2019 IEEE International Conference on Systems, Man and Cybernetics (SMC)*, Bari, Italy, 2019.

[59] F. Hafiz, A. Swain, and E. M. Mendes, "Two-dimensional (2D) particle swarms for structure selection of nonlinear systems," *Neurocomputing*, vol. 367, pp. 114–129, 2019.

[60] D. P. Solomatine and D. L. Shrestha, "AdaBoost.RT: a boosting algorithm for regression problems," in *2004 IEEE International Joint Conference on Neural Networks (IEEE Cat. No.04CH37541)*, pp. 1163–1168, Budapest, Hungary, 2004.

[61] F. Granata, F. Di Nunno, M. Najafzadeh, and I. Demir, "A stacked machine learning algorithm for multi-step ahead prediction of soil moisture," *Hydrology*, vol. 10, no. 1, p. 1, 2023.

[62] F. Saberi-Movahed, M. Najafzadeh, and A. Mehrpooya, "Receiving more accurate predictions for longitudinal dispersion coefficients in water pipelines: training group method of data handling using extreme learning machine conceptions," *Water Resources Management*, vol. 34, no. 2, pp. 529–561, 2020.

[63] M. Najafzadeh, M. R. Balf, and E. Rashedi, "Prediction of maximum scour depth around piers with debris accumulation using EPR, MT, and GEP models," *Journal of Hydroinformatics*, vol. 18, no. 5, pp. 867–884, 2016.

[64] M. Najafzadeh, A. Etemad-Shahidi, and S. Y. Lim, "Scour prediction in long contractions using ANFIS and SVM," *Ocean Engineering*, vol. 111, pp. 128–135, 2016.